

# Superconducting Parameters of Spinel $\text{CuRh}_2\text{S}_4$ under Pressure

M. ITO\*, A. TAIRA AND K. SONODA

Department of Physics and Astronomy, Graduate School of Science and Engineering, Kagoshima University,  
Kagoshima 890-0065, Japan

(Received February 16, 2016; revised version February 7, 2017; in final form April 14, 2017)

We investigated the magnetic properties of chalcogenide-spinel superconductor  $\text{CuRh}_2\text{S}_4$  under pressure and estimated the pressure dependence of the superconducting parameters. With increasing pressure, the superconducting transition temperature ( $T_c$ ), thermodynamic critical field ( $H_c$ ), upper critical field ( $H_{c2}$ ), penetration depth ( $\lambda$ ), and GL parameter ( $\kappa$ ) increase. Meanwhile, the lower critical field ( $H_{c1}$ ) is unchanged and the Ginzburg–Landau coherence length ( $\xi_{\text{GL}}$ ) is reduced by pressurization. The increasing value of  $\kappa$  indicates enhanced characteristics of the type-II superconductor  $\text{CuRh}_2\text{S}_4$ .

DOI: [10.12693/APhysPolA.131.1450](https://doi.org/10.12693/APhysPolA.131.1450)

PACS/topics: 74.70.Dd, 74.62.Fj, 74.25.Bt

## 1. Introduction

Chalcogenide spinels, which have the chemical formula  $\text{AB}_2\text{X}_4$  (A, B: transition metals, X: chalcogen), have a variety of attractive physical properties. The spinels have a cubic crystal structure with the space group  $Fd\bar{3}m$ . The characteristics of this structure are that A- and B-site ions are coordinated by four X-site ions to form a tetrahedron and by six X-site ions to form an octahedron, as shown in Fig. 1. Cu-based thiospinel tends to have a

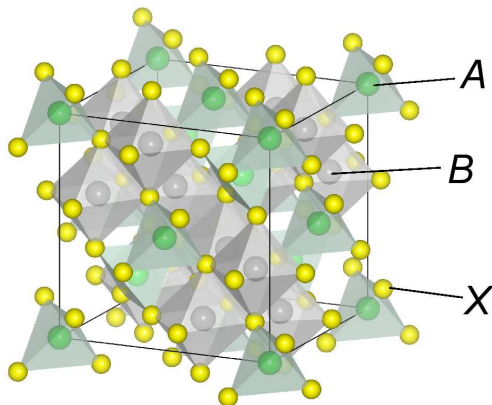


Fig. 1. Crystal structure of the spinel with the chemical formula  $\text{AB}_2\text{X}_4$ . The space group is  $Fd\bar{3}m$ .

mixed-valence state at the B site; i.e.,  $\text{B}^{3+}$  and  $\text{B}^{4+}$  coexist.  $\text{CuRh}_2\text{S}_4$  is a Bardeen–Cooper–Schrieffer (BCS) superconductor with a superconducting transition temperature  $T_c = 4.7$  K [1]. Hagino et al. investigated the electrical and thermodynamic properties of  $\text{CuRh}_2\text{S}_4$ , and estimated various superconducting parameters at ambient

pressure [2]. Tachibana recently obtained a value for the zero-temperature upper critical field,  $H_{c2}(0) = 33$  kOe, using low-temperature specific-heat measurements in a magnetic field [3]. The pressure dependence of  $T_c$  up to  $P = 2.2$  GPa for the spinels  $\text{LiTi}_2\text{O}_4$ ,  $\text{CuRh}_2\text{Se}_4$ , and  $\text{CuRh}_2\text{S}_4$  was investigated by Shelton et al. [4]. They reported that  $T_c$  increases proportionally to  $P$ , because of the enhancement of the Debye temperature,  $\theta$ .

Previously, one of the authors (M.I.) measured electric resistivity under pressure and reported the phenomenon of the pressure-induced transition of  $\text{CuRh}_2\text{S}_4$  from a superconductor to an insulator [5]. With increasing pressure,  $T_c$  initially increases to a maximum value of 6.4 K at 4.0 GPa and then slightly decreases. With further compression, superconductivity in  $\text{CuRh}_2\text{S}_4$  disappears abruptly at a critical pressure between 5.0 and 5.6 GPa, when it becomes an insulator. The origin of the pressure-induced transition from superconductor to insulator remains unclear. The present paper further investigates the effects of pressure on the superconducting properties of  $\text{CuRh}_2\text{S}_4$ , analyzes the magnetization of  $\text{CuRh}_2\text{S}_4$  under pressure, and estimates the pressure dependence of superconductivity parameters.

## 2. Experimental details

Polycrystalline  $\text{CuRh}_2\text{S}_4$  was prepared in a solid-state reaction. The temperature dependence of magnetization was measured using a Quantum Design MPMS SQUID magnetometer, in the temperature range from 2 to 10 K. The magnetization measurements were carried out after zero-field cooling to 2 K. Pressure up to 0.74 GPa was generated using a piston cylinder Be–Cu clamp cell that can be attached to the sample rod of the MPMS magnetometer [6]. The pressure in the low-temperature range was determined from the pressure dependence of the superconducting transition temperature of a small piece of Sn mounted in the pressure cell.

\*corresponding author; e-mail: [showa@sci.kagoshima-u.ac.jp](mailto:showa@sci.kagoshima-u.ac.jp)

### 3. Results and discussion

#### 3.1. Superconducting transition temperature, $T_c$

Figure 2a–c shows the temperature,  $T$ , dependence of magnetization divided by the applied field,  $M/H$ , of  $\text{CuRh}_2\text{S}_4$  for various magnetic fields and pressures. At all pressures,  $M/H$  dropped greatly at  $T_c$  in the weakest magnetic field ( $H = 50$  Oe). At  $P = 0.00$  GPa,  $T_{c\ p=0}$  was 4.5 K.

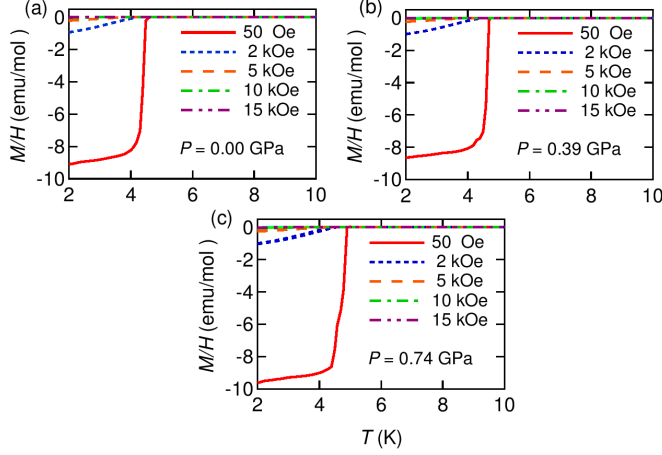


Fig. 2. Temperature dependence of magnetization divided by the applied field,  $M/H$ , of  $\text{CuRh}_2\text{S}_4$  for (a)  $P = 0.00$  GPa, (b)  $P = 0.39$  GPa, and (c)  $P = 0.74$  GPa.

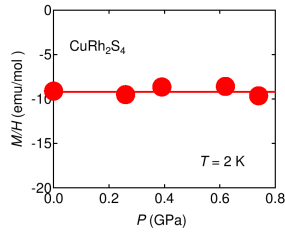


Fig. 3. Pressure dependence of  $M/H$  at  $T = 2$  K and  $H = 50$  Oe for  $\text{CuRh}_2\text{S}_4$ . The solid line is a visual aid.

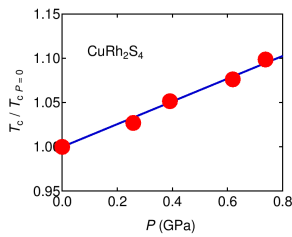


Fig. 4. Pressure dependence of the transition temperature normalized by the ambient pressure,  $T_c/T_{c\ P=0}$ , of  $\text{CuRh}_2\text{S}_4$ . The solid line shows the linear fitting result.

As shown in Fig. 3,  $M/H$  at  $H = 50$  Oe and  $T = 2$  K does not depend on  $P$  at  $0 \leq P \leq 0.74$  GPa. This means that the shielding volume fraction of  $\text{CuRh}_2\text{S}_4$  is insensitive to  $P$ .

Figure 4 shows the  $P$  dependence of  $T_c$  normalized by the value at  $P = 0.00$  GPa,  $T_c/T_{c\ p=0}$ . With pressurization,  $T_c/T_{c\ p=0}$  increases in proportion to  $P$  with an initial rate of  $d(T_c/T_{c\ p=0})/dP = 1.28 \times 10^{-1} \text{ GPa}^{-1}$ . When we employ  $T_{c\ p=0} = 4.5$  K,  $dT_c/dP$  is 0.57 K/GPa, which is close to the value ( $\approx 0.5$  K/GPa) reported by Shelton et al. [4]. This increase in  $T_c$  is due to increase of  $\theta$  as mentioned in Introduction. According to BCS theory,  $T_c$  can be described using  $\theta$ , electron–lattice interaction  $U$ , and the density of states at the Fermi energy  $D_{E_F}$  as  $T_c = 1.14\theta \exp(-1/UD_{E_F})$ . In general, with pressurization,  $\theta$  increases and  $D_{E_F}$  decreases owing to the Pauli exclusion principle. The increase in  $\theta$  and decrease in  $D_{E_F}$  increase and decrease  $T_c$ , respectively. As mentioned in Introduction, from the electrical resistivity measurement under pressure, we found that the  $P$  dependence of  $T_c$  changes from increase to decrease at  $P = 4.0$  GPa [5]. At  $P > 4.0$  GPa, the reduction of  $D_{E_F}$  might strongly affect the  $P$  dependence of  $T_c$  for  $\text{CuRh}_2\text{S}_4$ .

#### 3.2. Upper critical field, $H_{c2}$

Figure 5 shows the magnetization of  $\text{CuRh}_2\text{S}_4$ ,  $-4\pi M$ , as a function of the magnetic field at 2 K for various pressures. In the range of a weak magnetic field,  $-4\pi M$  increases linearly. After peaking at  $H$  of around 1200 Oe,  $-4\pi M$  decreases with  $H$  and reaches zero at around 2000–2500 Oe. For  $-4\pi M$  at various  $P$ , it is difficult to determine the zero-temperature upper critical field,  $H_{c2}(0)$ , directly from experimental results. We estimate the  $P$  dependence of  $H_{c2}(0)$  from the results for the lowest temperature ( $T = 2$  K),  $H_{c2}(2 \text{ K})$ .  $H_{c2}(2 \text{ K})$  can be obtained as the magnetic field at which  $-4\pi M = 0$ , as shown by the arrows in the main part of Fig. 5.

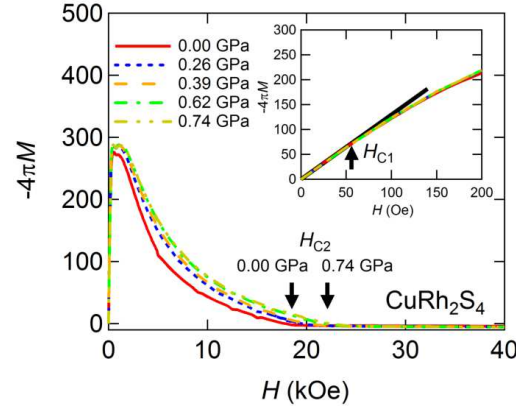


Fig. 5. Magnetic field dependence of magnetization (i.e.,  $M$ – $H$  curve) for  $\text{CuRh}_2\text{S}_4$  at  $T = 2$  K and various pressures. The arrows show the representative points of  $H_{c2}$  for  $P = 0$  and 0.74 GPa. The inset is the expanded plot of the low-field range. The arrow shows the point of deviation of  $M$  from linear dependence.

Figure 6 shows the  $P$  dependence of  $H_{c2}(2 \text{ K})$  normalized by the value at  $P = 0$  GPa,  $H_{c2}(2 \text{ K})/H_{c2}(2 \text{ K})_{P=0}$ . Previously, the  $P$  dependence of  $H_{c2}(0)$  was indirectly

estimated [7] using the Werthamer–Helfand–Hohenberg (WHH) formula [8],  $H_{c2}(0) = 0.693T_c \left| \frac{dH_{c2}}{dT} \right|_{T_c}$ ; the obtained  $H_{c2}(0)/H_{c2}(0)_{P=0}$  is also plotted in the figure. The  $P$  responses of  $H_{c2}(2\text{ K})/H_{c2}(2\text{ K})_{P=0}$  and  $H_{c2}(0)/H_{c2}(0)_{P=0}$  are similar and we consider  $H_{c2}(2\text{ K})/H_{c2}(2\text{ K})_{P=0} = H_{c2}(0)/H_{c2}(0)_{P=0}$ . We obtained the initial increasing rate of  $d(H_{c2}(0)/H_{c2}(0)_{P=0})/dP = 2.73 \times 10^{-1} \text{ GPa}^{-1}$  from the solid line in Fig. 6. When we use  $H_{c2}(0) = 33 \text{ kOe}$ , obtained from the specific-heat measurement under a magnetic field [3],  $H_{c2}(0)$  reaches  $\approx 40 \text{ kOe}$  at  $P = 0.74 \text{ GPa}$ .

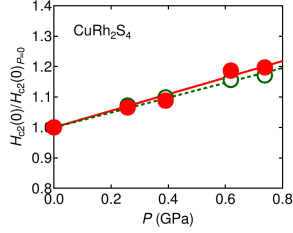


Fig. 6. Pressure dependence of the zero- $T$  upper critical field normalized by ambient pressure,  $H_{c2}(0)/H_{c2}(0)_{P=0}$ , estimated from the WHH formula (open circles) and from the  $M$ - $H$  curves at 2 K (closed circles). The solid and dotted lines show linear fitting results.

### 3.3. Ginzburg–Landau coherence length, $\xi_{GL}$

The Ginzburg–Landau (GL) coherence length,  $\xi_{GL}$ , can be obtained from the relation

$$\xi_{GL} = \left( \frac{\Phi_0}{2\pi H_{c2}(0)} \right)^{1/2}, \quad (1)$$

where  $\Phi_0 (= 2.07 \times 10^{-7} \text{ G cm}^2)$  is the magnetic flux quantum. The pressure dependence of  $\xi_{GL}$  is estimated using Eq. (1) and the  $P$  dependence of  $H_{c2}(0)$ . Figure 7 shows  $\xi_{GL}$  normalized by the value of ambient pressure,  $\xi_{GL}/\xi_{GL P=0}$ , as a function of  $P$ . With increasing  $P$ ,  $\xi_{GL}/\xi_{GL P=0}$  decreases with an initial rate of  $-1.10 \times 10^{-1} \text{ GPa}^{-1}$ . When  $H_{c2}(0) = 33 \text{ kOe}$  [3] is adopted,  $\xi_{GL P=0} = 93 \text{ \AA}$  is estimated, and  $\xi_{GL}$  reduces to  $85 \text{ \AA}$  at  $P = 0.74 \text{ GPa}$  with pressurization.

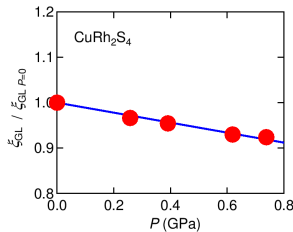


Fig. 7. Pressure dependence of the GL coherence length normalized by ambient pressure,  $\xi_{GL}/\xi_{GL P=0}$ , of  $\text{CuRh}_2\text{S}_4$ . The solid line shows the linear fitting result.

### 3.4. Penetration depth, $\lambda$ , GL parameter, $\kappa$ , lower critical field, $H_{c1}$ , and thermodynamic critical field, $H_c$

Penetration depth,  $\lambda$ , is related to the zero-temperature thermodynamic critical field,  $H_c(0)$ , by

$$H_c(0) = \frac{\Phi_0}{2\sqrt{2}\pi\lambda\xi_{GL}}. \quad (2)$$

$\lambda$  at  $P = 0 \text{ GPa}$ ,  $\lambda_{P=0}$ , is  $3558 \text{ \AA}$ , when using  $H_c(0)_{P=0} = 704 \text{ Oe}$  reported by Hagino et al. [2]. Meanwhile, the zero-temperature lower critical field,  $H_{c1}(0)$ , is expressed as

$$H_{c1}(0) = \frac{\Phi_0}{4\pi\lambda^2(0)} \ln \kappa, \quad (3)$$

where the GL parameter  $\kappa$  is

$$\kappa = \frac{\lambda}{\xi_{GL}}. \quad (4)$$

We get  $H_{c1}(0) = 47 \text{ Oe}$  using  $\lambda_{P=0} = 3558 \text{ \AA}$  and  $\xi_{GL P=0} = 93 \text{ \AA}$  from Eqs. (3) and (4). It is difficult to measure  $H_{c1}(0)$  accurately from  $M$ - $H$  curves obtained in experiments. We estimated the lower critical field at  $T = 2 \text{ K}$ ,  $H_{c1}(2 \text{ K}) = 55 \text{ Oe}$ , as the point at which  $-4\pi M$  deviates from having a linear dependence on  $H$  as shown by an arrow in the inset of Fig. 5. This value of  $H_{c1}(2 \text{ K})$  is close to  $H_{c1}(0)$  ( $\approx 47 \text{ Oe}$ ) obtained above. Because  $H_{c1}(2 \text{ K})$  is insensitive to  $P$  up to  $0.74 \text{ GPa}$ , we consider that  $H_{c1}(0)$  is also constant for varying  $P$ . From numerical calculations using Eq. (3), (4) and the  $P$  dependence of  $\xi_{GL}$  (Fig. 7), the  $P$  dependence of  $\lambda$  can be obtained.

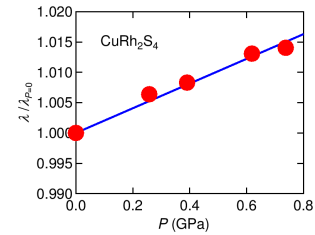


Fig. 8. Pressure dependence of the penetration depth normalized by ambient pressure,  $\lambda/\lambda_{P=0}$ , of  $\text{CuRh}_2\text{S}_4$ .

Figure 8 shows the  $P$  dependence of  $\lambda/\lambda_{P=0}$ . With increase of  $P$ ,  $\lambda/\lambda_{P=0}$  increases with an initial rate of  $2.04 \times 10^{-2} \text{ GPa}^{-1}$ .  $\kappa$  at  $P = 0 \text{ GPa}$ ,  $\kappa_{P=0}$ , has a value of 38 according to Eq. (4). The  $P$  dependence of  $\kappa$  is obtained from the results presented in Figs. 7 and 8. Figure 9 shows that  $\kappa/\kappa_{P=0}$  increases monotonically against  $P$  with an initial rate of  $1.33 \times 10^{-1} \text{ GPa}^{-1}$ . It is well known that superconductors are classified as type-I superconductors for  $\kappa < 1/\sqrt{2}$  and type-II superconductors for  $\kappa > 1/\sqrt{2}$ .  $\text{CuRh}_2\text{S}_4$  is a typical type-II superconductor with  $\kappa_{P=0} = 21 \div 38$  [2]. The increasing value of  $\kappa/\kappa_{P=0}$  means that the characteristics of the type-II superconductor of this system are further enhanced by pressurization. We finally estimated the  $P$  dependence of  $H_c(0)$  using Eq. (2), as shown in Fig. 10.  $H_c(0)/H_c(0)_{P=0}$  increases with pressurization at an initial rate of  $9.62 \times 10^{-2} \text{ GPa}^{-1}$ .

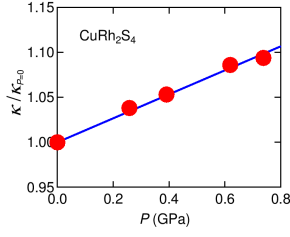


Fig. 9. Pressure dependence of the GL parameter normalized by ambient pressure,  $\kappa/\kappa_{P=0}$ , of  $\text{CuRh}_2\text{S}_4$ . The solid line shows the linear fitting result.

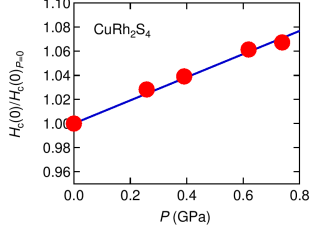


Fig. 10. Pressure dependence of the zero- $T$  thermodynamic critical field normalized by ambient pressure,  $H_c(0)/H_c(0)_{P=0}$ , of  $\text{CuRh}_2\text{S}_4$ . The solid line shows the linear fitting result.

#### 4. Conclusion

We investigated the magnetization of spinel superconductor  $\text{CuRh}_2\text{S}_4$  under pressure and obtained the pressure dependence of superconducting parameters.  $T_c$  increases at the rate  $d(T_c/T_{c\ P=0})/dP = 1.28 \times 10^{-1} \text{ GPa}^{-1}$ . We also obtained the initial rates of change with pressure  $d(H_c(0)/H_c(0)_{P=0})/dP = 9.62 \times 10^{-2} \text{ GPa}^{-1}$ ,  $d(H_{c2}(0)/H_{c2}(0)_{P=0})/dP = 2.73 \times 10^{-1} \text{ GPa}^{-1}$ ,  $d(\lambda/\lambda_{P=0})/dP = 2.04 \times 10^{-2} \text{ GPa}^{-1}$ ,  $d(\kappa/\kappa_{P=0})/dP = 1.33 \times 10^{-1} \text{ GPa}^{-1}$ , and  $d(\xi_{GL}/\xi_{GLP=0})/dP = -1.10 \times 10^{-1} \text{ GPa}^{-1}$ . Meanwhile,  $H_{c1}(0)$  does not change with pressurization. The pressure dependence of superconducting parameters of  $\text{CuRh}_2\text{S}_4$  is summarized in Table I. Because  $(\kappa/\kappa_{P=0})$  increases with pressurization, the superconducting state of  $\text{CuRh}_2\text{S}_4$  enhances the features of a type-II superconductor with pressurization. More detailed pressure studies in a higher pressure range are needed to clarify the origin of the pressure-induced transition of this system from superconductor to insulator.

TABLE I

Superconducting parameters of  $\text{CuRh}_2\text{S}_4$  under pressure.

Parameter	Initial change rate with pressure [ $\text{GPa}^{-1}$ ]
$T_c/T_{c\ P=0}$	0.128
$(M/H)/(M/H)_{P=0}$	no change
$H_c(0)/H_c(0)_{P=0}$	0.0962
$H_{c1}(0)/H_{c1}(0)_{P=0}$	no change
$H_{c2}(0)/H_{c2}(0)_{P=0}$	0.273
$\xi_{GL}/\xi_{GLP=0}$	-0.11
$\lambda/\lambda_{P=0}$	0.0204
$\kappa/\kappa_{P=0}$	0.133

#### Acknowledgments

The figure of the crystal structure was drawn with VESTA [9].

#### References

- [1] N.H. Van Maaren, G.M. Schaeffer, F.K. Lotgering, *Phys. Lett. A* **25**, 238 (1967).
- [2] T. Hagino, Y. Seki, N. Wada, S. Tsuji, T. Shirane, K. Kumagai, S. Nagata, *Phys. Rev. B* **51**, 12673 (1995).
- [3] M. Tachibana, *Solid State Commun.* **152**, 849 (2012).
- [4] R.N. Shelton, D.C. Johnston, H. Adrian, *Solid State Commun.* **20**, 1077 (1976).
- [5] M. Ito, J. Hori, H. Kurisaki, H. Okada, A.J. Perez Kuroki, N. Ogita, M. Udagawa, H. Fujii, F. Nakamura, T. Fujita, T. Suzuki, *Phys. Rev. Lett.* **91**, 077001 (2003).
- [6] Y. Uwatoko, T. Hotta, E. Matsumoto, H. Mori, T. Ohki, J.L. Sarrao, J.D. Thompson, N. Mori, G. Oomi, *Rev. High Pressure Sci. Technol.* **7**, 1508 (1998).
- [7] M. Ito, K. Ishii, F. Nakamura, T. Suzuki, *AIP Conf. Proc.* **850**, 627 (2006).
- [8] N.R. Werthamer, E. Helfand, P.C. Hohenberg, *Phys. Rev.* **147**, 295 (1966).
- [9] K. Momma, F. Izumi, *J. Appl. Crystallogr.* **44**, 1272 (2011).